



## SPE/Petroleum Society of CIM/CHOA 78975

### Geomechanics and wellbore stability design of an offshore horizontal well, North Sea

Patrick M. Collins, SPE, CIM, CHOA, Petroleum Geomechanics Inc.

Copyright 2002, SPE ITOHOS/ICHWT conference.

This paper was prepared for presentation at the SPE International Thermal Operations and Heavy Oil Symposium and International Horizontal Well Technology Conference held in Calgary, Alberta, Canada, 4-7 November 2002.

This paper was selected for presentation by an SPE ITOHOS/ICHWT Program Committee following review of information contained in an abstract submitted by the author(s). Contents of the paper, as presented, have not been reviewed by the Society of Petroleum Engineers, the Petroleum Society of CIM/CHOA and are subject to correction by the author(s). The material, as presented, does not necessarily reflect any position of the Society of Petroleum Engineers, the Petroleum Society of CIM/CHOA, its officers, or members. Papers presented at SPE ITOHOS/ICHWT meetings are subject to publication review by Editorial Committees of the Society of Petroleum Engineers. Electronic reproduction, distribution, or storage of any part of this paper for commercial purposes without the written consent of the Society of Petroleum Engineers is prohibited. Permission to reproduce in print is restricted to an abstract of not more than 300 words; illustrations may not be copied. The abstract must contain conspicuous acknowledgment of where and by whom the paper was presented. Write Librarian, SPE, P.O. Box 833836, Richardson, TX 75083-3836, U.S.A., fax 01-972-952-9435.

#### Abstract

This paper describes a comprehensive geomechanical assessment of the P2-NE Field in the North Sea. The objective was to review the available core, log, and drilling data to characterize the geomechanical performance of the P2-NE Field in order to explain observed behaviour, and extrapolate this to future drilling, particularly for Well P2-NE-2 Horizontal. This study focussed on the inclined Well P2-NE-2 Pilot, which was drilled specifically to obtain reservoir data for the subsequent horizontal well. The geomechanical analysis is based upon the general geological setting, deductions made from field data, and geomechanical core tests. Wellbore stability analyses were conducted, using the mechanical properties and regional stresses as input.

Geomechanical tests and petrophysical logs were used to obtain realistic profiles of mechanical properties. Anomalously, the reservoir mudstones were of considerable strength, exceeding the strengths of the sandstones. Weak zones were found in the sandstone that would be stable while drilling if an adequate mud weight were used. These zones would likely be sand producers during production. This is because the rock stresses would continue to increase, due to the continued pressure decline during depletion.

To obtain stress data, a minifrac test from an adjacent field was analyzed. This provided the breakdown pressure, fracture propagation pressure, the ISIP, and most importantly the fracture closure pressure. The principal horizontal stress orientations were determined from borehole breakout analyses, and compared to residual strain relaxation tests on core. Other observed borehole elongations included wellbore washouts and keyseating. Finally, a stability analysis was

conducted for the horizontal well, in order to assess the effect of increasing the mud weight.

#### Introduction

The primary objective was to determine the minimum mud weights required for wellbore stability during drilling, and these were found to be considerably less than those predicted without a geomechanics analysis. Fracture gradients set a maximum for the ECD. Zones with high sanding potentials were identified, based on the rock strength analyses.

#### Geology

**Structural Geology.** The P2-NE Reservoir is in the northeast corner of Block P2a in the North Sea, as seen in **Figure 1**. The reservoir is within a horst structure formed between normal faults and is similar to other reservoirs in the vicinity, including the P2-SE reservoir located to the south.

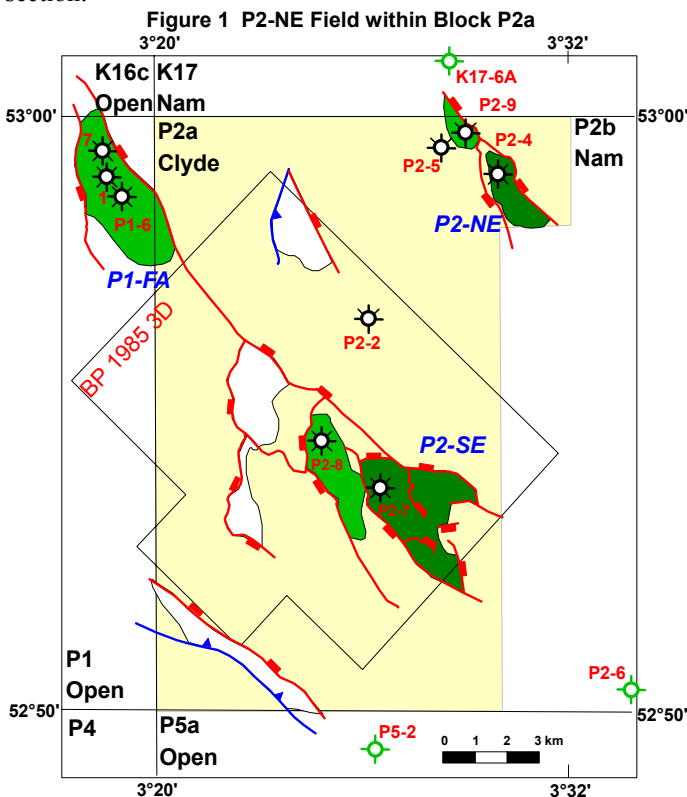
The P2-NE Reservoir is structurally bounded on two sides by two major normal faults striking NW-SE. These faults converge towards the northwest, thereby pinching-off the reservoir. Towards the southeast the Rotliegend Formation deepens, and the resultant wedge of Rotliegend forms the trap for the gas in the reservoir.

**Stratigraphy.** This reservoir is comprised of sandstones and mudstones. Surprisingly, the mudstones appear to be stronger and stiffer than the sandstones, as determined from an analysis of sonic logs and geomechanical core tests conducted for this study.

The stratigraphy of P2-NE at the reservoir level is shown in **Figure 2**. A NW-SE cross-section is displayed, along with the Well P2-NE-2 Pilot and Well P2-NE-2 Horizontal trajectories. Since the horizontal length of the horizontal well is approximately 1.5 km, there is no vertical exaggeration in this figure, i.e. the apparent slopes and angles are real.

The 244mm (9 5/8") casing shoe was set within the Zechstein anhydrite, from which the Pilot well was advanced at an inclination of 55°. As shown on the figure, this inclined pilot well intersected all Rotliegend zones. In general, the Rotliegend rocks are sandstones with zone boundaries often delimited by shales. The current gas:water contact is the base of the gas:water transition zone, shown as a horizontal band within dashed lines. Normal faults present in the P2-NE Field were not intersected by the planned horizontal well trajectory. The dominant normal faulting pattern strikes parallel to this

cross-section; therefore, faulting is not seen in this cross-section.

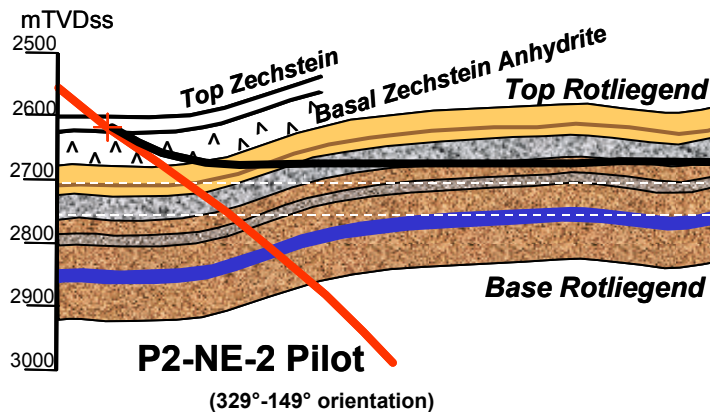


### In Situ Stress State

The absence of normal faulting in this cross-section (Fig. 2) suggests that the magnitudes of the two horizontal in-situ stresses are dissimilar, as would be expected. The dominant faulting strike is NW-SE. These faults may exist to accommodate the high curvatures in the Top Rotliegend, perpendicular to this cross-section (not shown). The post-depositional draping of these formations over the stronger carbonate underburden suggests that deeper movements are controlling the deformations at the reservoir level.

Normal faulting is indicative of extensional strains in the rocks: at higher strains, the rock has faulted rather than

**Figure 2** Cross-section through P2-NE Field with well trajectories,



strained. As a result of this extension, the fracture gradient might be expected to be less than a normal gradient predicted using solid mechanics, such as the Eaton (1969) equation<sup>1</sup>:

$$\sigma_h = \frac{\nu}{1-\nu} (\sigma_v - p_f) + p_f \quad [1]$$

where

$\sigma_h$  = horizontal stress (i.e., fracture gradient)

$\nu$  = Poisson's ratio

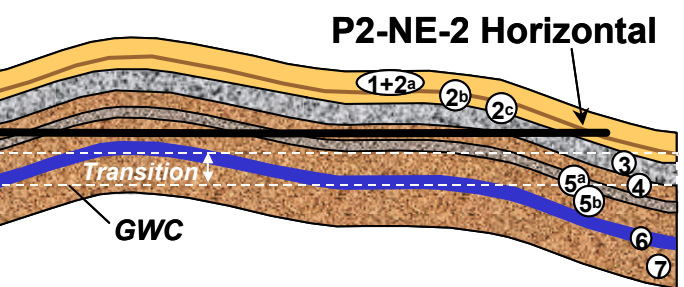
$\sigma_v$  = vertical stress

$p_f$  = formation fluid pressure

Stresses in the perpendicular NE-SW direction should be lower than this, given the dominant NW-SE normal fault pattern and the anisotropic stresses, evident from borehole breakout analyses. Methods exist to predict the stress range to initiate faulting<sup>2</sup>; however, subsequent strains and faulting itself modify those stresses to the point that these initiating stresses may no longer reflect the current stresses. Eaton's equation (Eq'n. 1) generally provides a good first-order estimate of the minimum horizontal stress in a depositional basin like the North Sea.

The presence of anhydrite salt above the reservoir does not appear to have affected the stresses in the Rotliegend Formation. In geologic time, the salt's mechanical behaviour is like a fluid in that it is less capable of supporting shear stresses, and will deform instead. As a result, stresses in salts can become lithostatic, with all stresses being equal to the overburden stress. This provides a constant stress upper boundary to the Rotliegend. This is less restricting than the case of a non-salt rock, which would provide more resistance to any differential upward movement of the reservoir.

**Borehole Breakouts.** When a borehole is drilled into a rock mass, the initial stress state in the rock is altered in the vicinity of the borehole due to the removal of the support from the drilled rock, and its replacement with an internal mud pressure. These changes in stress result in new stress states in the rock that may exceed the strength of the rock. In such cases the rock will fail in some locations, typically in fractured zones at the borehole wall that are diametrically opposed. If this failed rock is removed, an elongated borehole cross-section, or "breakout", remains (Figure 3). The orientation of this elongated borehole is normal to the direction of the



maximum horizontal stress.

Breakout analyses were performed on available caliper data from Wells P2-4 and P2-5 in the P2-NE Reservoir. In addition, a borehole geometry report was available for Well P2-NE-2 Pilot. In Wells P2-4 and P2-5, borehole breakouts

were the dominant forms of borehole elongation. Keyseats were present in Well P2-NE-2 Pilot, which was expected, given the 55° well inclination.

**Breakout Analysis of Well P2-4.** Oriented caliper data were available for the interval 2745-3013 mMD. Well inclinations increase from 9° to 20° over this interval, at a constant azimuth of 150° (**Figure 4**).

Breakouts were the predominant form of borehole elongation over the interval, although there are two instances of hole enlargement that appear to be due to washout. The depth of breakout (i.e. overgauge) is not very high. Maximum caliper readings are typically in the 7.5" to 8.5" range, with some isolated occurrences exceeding this. Calipers in the transverse direction are either at gauge or are slightly greater than gauge. This combination of features is indicative of breakouts: the rock has high localized stress concentrations at the wellbore wall that are compounded by the lack of support with the low mud weights. Fortunately, the damaged wellbore is strong enough to remain stable. Breakouts are very distinctive, and have a consistent orientation of 040°-220°. Based on the borehole breakout analysis, the maximum horizontal stress orientation is 130°-310°.

The two instances of washout were from 2870m to 2895mMD, and from 2925m to 2955mMD. Here, the hole enlargement in both caliper directions is indicative of washout. However, the rough caliper trace of the minor caliper is more typical of stress-related features, i.e., breakout. Sometimes this roughness can be correlated with the gamma ray trace, indicating either a difference in rock strength or erodability, but the gamma ray trace was unavailable. Within the washouts the azimuth of the smoother larger caliper trace happens to coincide with the hole azimuth (130° vs. 150°). Thus, there may be some secondary hole erosion due to the mechanical friction of the drill string against the rock ("keyseating"). At these angles of inclination (9° to 20°) some mechanical abrasion effects may be expected on the low side of the hole, resulting in keyseating features. Keyseating will tend to occur where the formation is softer, the inclination is highest, or where the狗leg curvature is greatest.

**Breakout Analysis of Well P2-5.** Oriented caliper data were available for the interval 3275-3715 mMD. Well inclinations varied from 15° to 20° over this interval, at a decreasing well azimuth of 215° to 200°.

An analysis was done, similar to that of Well P2-4. Breakouts were the predominant form of borehole elongation over the interval, although some keyseating effects may have been evident. Breakouts are very clear, and as with Well P2-4, have a consistent orientation of 040°-220° which indicates a maximum horizontal stress orientation of 130°-310°.

**Breakout Rosettes.** Orientations of breakouts were extremely consistent within Wells P2-4 and P2-5, as seen in the summary rosettes of **Figure 5** and **Figure 6**. Some washout was seen in Well P2-4, and this is typically seen at right angles to the breakouts. This may be because the caliper tool is often locked-in to the breakout orientation before a washout, and is less likely to rotate within the washout due to the combined effects of the roughened wellbore surface and the increased

**Figure 3 Borehole Breakout Schematic**

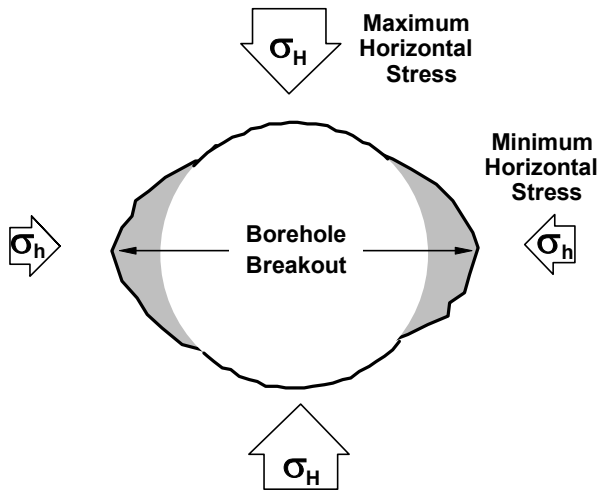
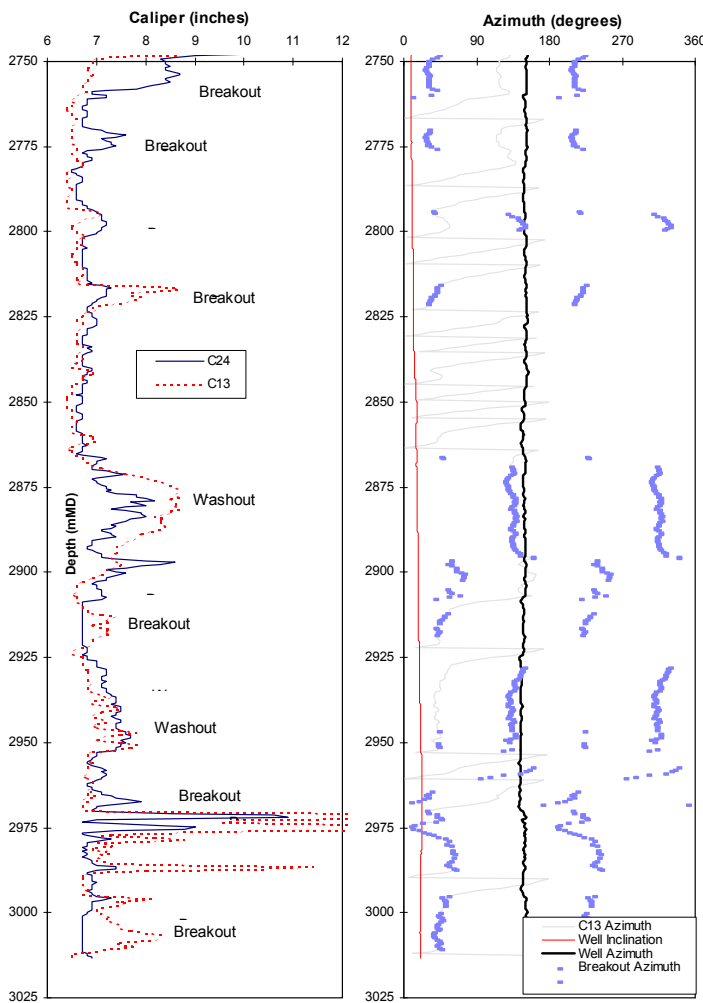


**Figure 4 Breakout Analysis of Well P2-4**



torsional resistance of the outstretched caliper arms. Also, as the washout corresponds to the well azimuth, there may be a keyseat effect superimposed on the washout.

As inferred from the  $040^\circ\text{--}220^\circ$  breakout orientations of Wells P2-4 and P2-5, the orientation of the major horizontal stress is  $130^\circ\text{--}310^\circ$ .

**Borehole Image of Well P2-NE-2 Pilot.** An ultrasonic borehole imager (UBI/DSI/GR) log was run in the 8.5" section over the interval 2935 to 3465 mMD. Well inclinations decrease from  $54^\circ$  to  $41^\circ$  over this interval, and the well azimuth was south south-east.

Figure 5

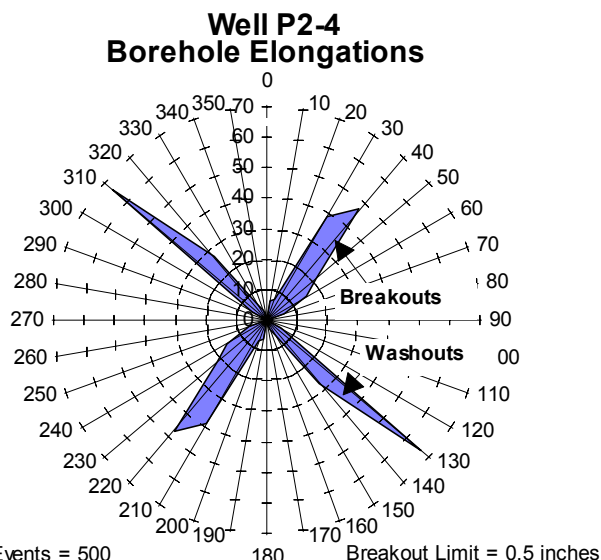
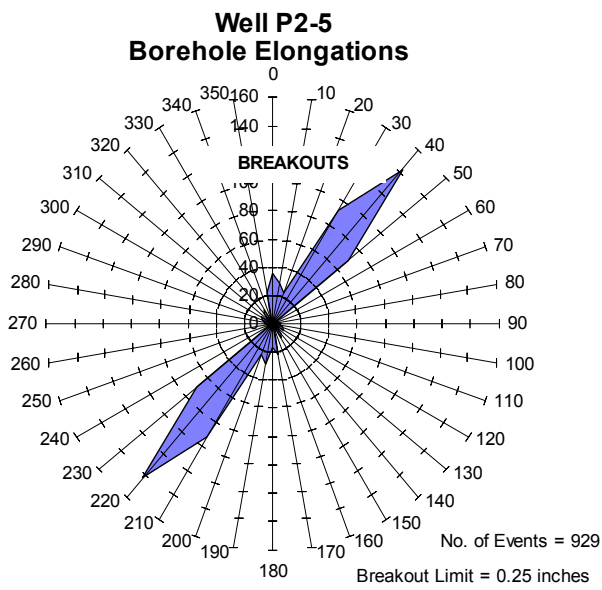


Figure 6



As one should expect in this high-angle pilot well, the predominant borehole elongations are keyseating due to the drillstring lying on the bottom of the well, with breakouts in the horizontal plane. These breakouts only confirm that the vertical stress is the major principal stress. Breakouts from highly inclined wells are predominantly affected by the vertical stress; thus, deducing the orientation of principal horizontal stresses from subtle changes in breakout azimuths in high-angle wells ( $>20^\circ$ ) is very suspect.

**Residual Strain Relaxation.** (RSR) is a technique used to determine the magnitude and direction of core strains. These strains are a result of re-adjustments in grain stresses, as locked-in stresses are reduced, when some core material is removed. A cylinder of whole core is prepared by polishing one end: strain gauge rosettes are attached to it, and strains are measured as the cylinder is cut in half. Subsequent cuts result in additional strains. The core is left to equilibrate to obtain "eventual" strains.

The method presumes that the direction of the principal maximum strain is the direction of the *in situ* principal maximum stress. It also assumes that the rock has no directionality in its material properties; an assumption that can be a fair approximation in the horizontal plane.

Two sandstone core intervals were selected for this technique. The most consistent result provided a maximum principal strain orientation averaging  $100^\circ\text{--}280^\circ$ . As this was an inclined core, the orientation was corrected to a horizontal orientation of  $112^\circ\text{--}292^\circ$ . This is in fair agreement with the borehole breakout result of  $130^\circ\text{--}310^\circ$ . However, the breakout result remains the superior result.

#### Horizontal Stress Magnitudes in the P2-NE Reservoir

The horizontal stress magnitudes in the P2-NE Reservoir are unlikely to be very high:

1. A minifrac test on Well P2-7 in the nearby P2-SE Reservoir provided an expected fracture closure stress.
2. The formations were reportedly normally pressured.
3. In an area of normal faulting, the magnitude of the minimum horizontal stress should be less than that predicted using Eaton's equation (Eq'n. 1).

It was assumed that there had been no subsequent recompression of the rock and no major tectonic activity that would significantly change the current *in situ* stresses from those that originally created the faulting system. The extremely high consistency between the principal horizontal stress orientations and the fault strikes supports this.

#### RSR determination of the Horizontal Stress Ratio

RSR techniques may be used to determine the relative magnitudes of the two horizontal stresses. This is done by assuming that the two principal strains are in the same proportion as the two horizontal principal effective stresses. However, in examining the eventual strains from the two specimens, it was clear that the strain ratios were too varied to determine the horizontal stress ratio. This variability may mean that the results of the RSR technique should be taken with a degree of caution, but it does not necessarily invalidate

the principal stress orientations as these are less sensitive to the strain magnitudes.

**Mud Losses and LOTs.** Indications of the minimum horizontal stress magnitude can be obtained from drilling data, e.g.: incidence of mud losses during drilling, and leak-off tests (LOTs) taken to leak-off. No useful data were available for the P2-NE Field at the reservoir depth. An attempt to obtain stress data in Well P2-NE-2 Pilot was made at the 9 5/8" casing shoe. The extended leakoff test (XLOT) procedure was recommended, as per Kunze and Steiger (1991, 1992)<sup>3,4</sup>. Unfortunately, there were difficulties in the field so the test was not conducted.

**P2-7 Minifrac Test.** Two minifrac's that were done in Well P2-7 in the nearby P2-SE Reservoir. A coarse plot of the DST2 test in Rotliegend Zone 1 was available, from which the minifrac portion was reproduced (**Figure 7**).

DST2 was performed over an interval from 3305-3334mMD. The well was essentially vertical, with an inclination of 7° at depth. The formation fluid gradient found

Figure 7 Well P2-7 DST2 Minifrac Pressure vs. Time

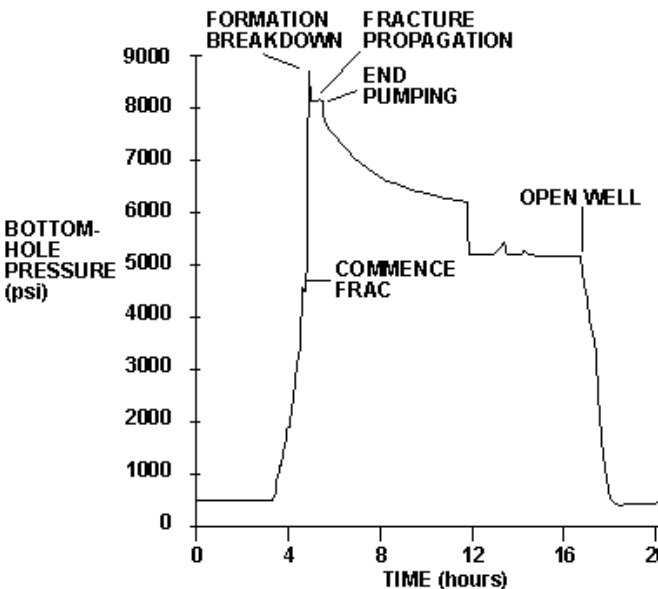


Table 1 Summary of P2-7 DST2 Minifrac Results

| Fracture Parameter             | Bottomhole Pressure (psi) | Gradient (psi/ft) | Gradient (S.G.) |
|--------------------------------|---------------------------|-------------------|-----------------|
| Formation Breakdown            | 8800                      | 0.81              | 1.87            |
| Fracture Propagation           | 8250                      | 0.76              | 1.76            |
| Instantaneous Shut-in Pressure | 7800                      | 0.72              | 1.66            |
| Formation Closure, root-time   | 6600                      | 0.61              | 1.40            |
| Formation Closure, G-function  | 6800                      | 0.63              | 1.45            |
| Formation Closure, Horner plot | 6700                      | 0.62              | 1.43            |
| Net Fracture Pressure          | 450                       |                   |                 |

gradients assume TVD at top of perforations of 3305m = 10,843 feet

from DST1 in Zone 3 was 1.09 SG; no value was stated for DST2, so it was assumed to be identical.

The reported fracture breakdown pressure was 0.85 psi/ft (1.96 SG) although the plot indicated a value of 8800 psi or 0.81 psi/ft (1.87 SG). The fracture propagation pressure was 8250 psi or 0.76 psi/ft (1.76 SG). There was no analysis of pressure falloff because it was stated that the zone was underproductive and not worthy of intensive examination. No other data were found.

In this study, the subsequent analyses of the pressure falloff data indicated a fracture closure stress of 6600 to 6800 psi (**Table 1**). This fracture closure stress provided the best measurement of the minimum horizontal stress.

### Laboratory Geomechanical Properties

The tests selected included unconfined compression strength (UCS), thick-walled cylinder (TWC), triaxial, and residual strain, and paleomagnetism. The purposes of these tests were to calibrate log-derived profiles, obtain strength parameters for stability modelling, determine the effect of core orientation on strength, and to determine the orientation of the maximum principal stress as a check on borehole breakout studies.

**Core Selection and Testing.** Core samples from Well P2-NE-2 Pilot were selected on the basis of being representative of the most typical facies within the cored interval: Rotliegend Zones 1 to 5a. The samples were selected for testing on the basis of log-derived UCS values. In addition, a suspected weak zone at 3134mMD (core depth) was added to the program.

Testing was done on specimens cored from the core sample. UCS tests were done on plugs from all test depths. More intensive testing was selected on core from Zone 3 and a massive mudstone in Zone 5a with bedding features, on the basis that they were best representative of the P2-NE Reservoir. In addition to the UCS testing, these samples were also tested for oriented UCS, confined compressive strength (triaxial), Young's modulus, Poisson's ratio, and thick-walled cylinder (TWC) tests. One shear box test was done.

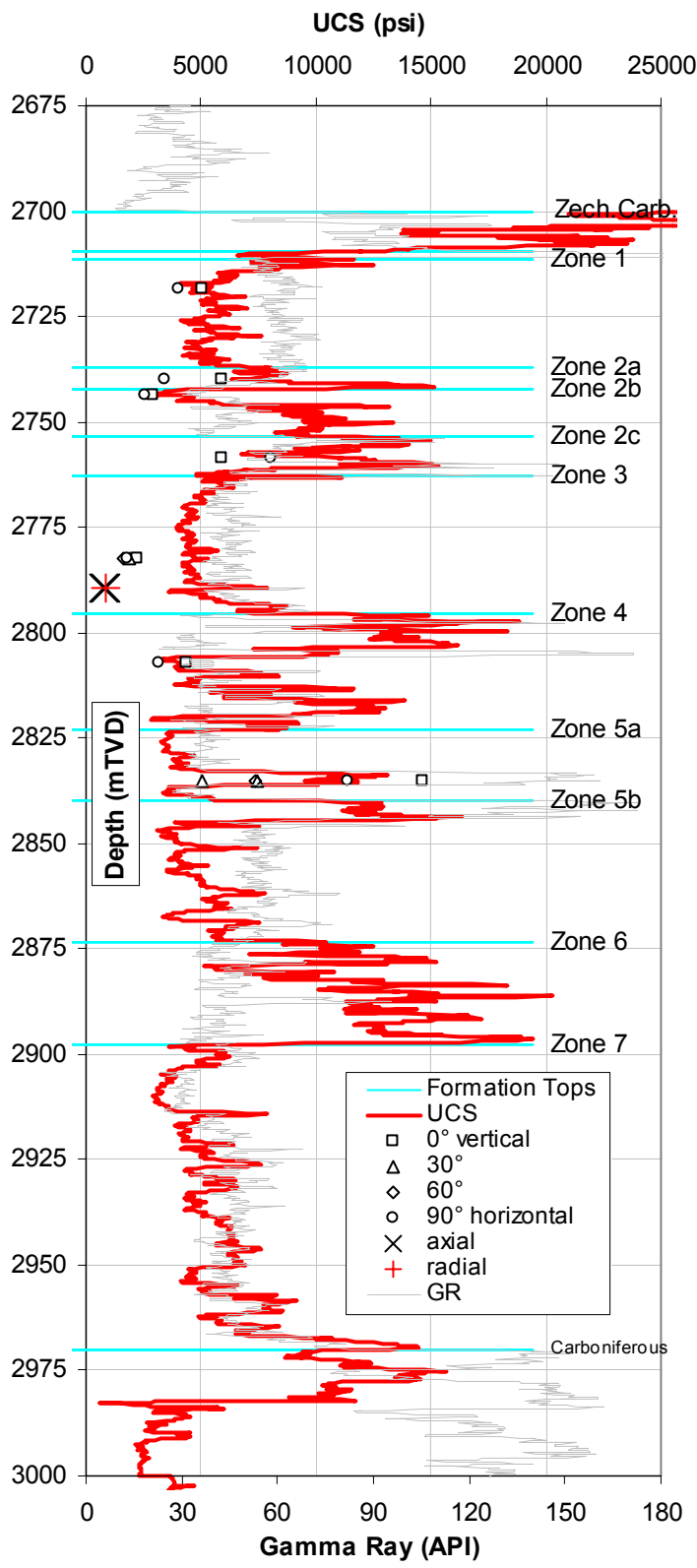
**Unconfined Compressive Strength.** UCS tests were performed on plugged core specimens 1-inch in diameter. The P2-NE specimens appeared to be stiff, therefore brittle failure was expected.

Specimens can be cored at any orientation with respect to bedding, in order to determine if there is any effect of bedding on strength. Strengths are typically highest perpendicular to bedding. This is because the natural deposition and subsequent compaction of sediments results in a stronger, more stable structure perpendicular to bedding.

The P2-NE core was tested parallel and perpendicular to bedding, and in some cases at 0°, 30°, 60°, and 90° to bedding. **Figure 8** shows a plot of a log-derived UCS profile, plus the laboratory values of compressive strengths from oriented specimens. Three features are immediately apparent:

1. there is a broad range of strengths, varying from 2,000 psi to 20,000 psi for log-derived values, and from 746 psi to 14,644 psi for laboratory values.

**Figure 8 Well P2-NE-2 Pilot Log-Derived Unconfined Compressive Strength**



2. the sandstone specimens were isotropic with no strong dependence on specimen orientation
3. the mudstone specimens were anisotropic, with a strong dependence on specimen orientation

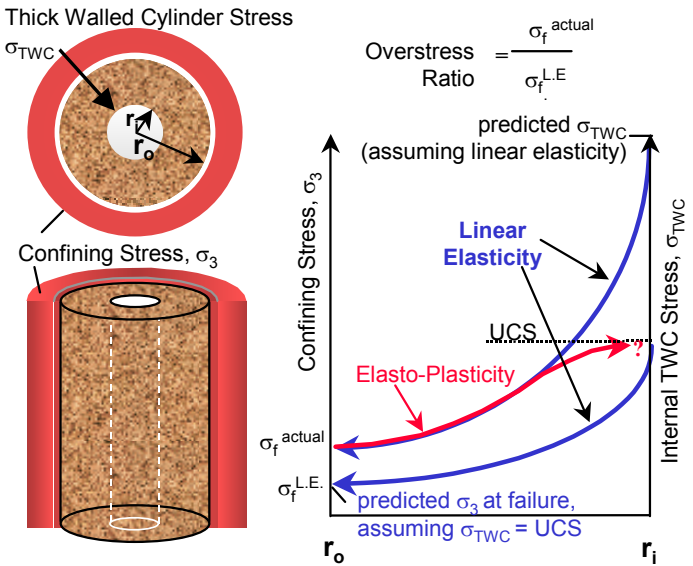
There is some correlation between rock strength and gamma ray, with similar strengths exhibited within each layer. Unusually, the high gamma ray intervals have significantly higher strengths than the sandstone units. The mudstone core was greyish-pink in colour, was unusually hard, and had a glossy appearance, but was not acid-reactive. This core was speculated to be siliceous, although no mineralogical analyses were performed to confirm this. The high mudstone strength was beneficial to wellbore stability since shales are usually weaker than sandstones at downhole conditions.

The weakest specimens are notable, particularly the friable sandstone at 2789.6 mTVD. Two axial specimens and one radial specimen were tested: UCS values were tightly grouped from 746 to 834 psi. With sufficient mud weight and mudcake build-up during drilling, this zone should remain stable. However, this is undoubtedly an interval of potential sand production as the reservoir pressure decreases and the stress on the rock increases. Slightly higher values were found for typical Zone 3 sandstone (1657 to 2197 psi). Again, this zone represented a potential for sand production with continued depletion.

**Thick-Walled Cylinder Tests.** TWCs are right circular cylinders approximately 3 inches in height and 1.5 inches in diameter, with a co-axial 0.5-inch diameter hole drilled through the sample, as shown in **Figure 9**. A confining stress is applied to the outside surface while the interior surface is at zero pressure. Due to the geometry of the sample and loading, there is a multiplier effect on the stresses within the rock. The outside of the specimen is subjected to the applied radial stress and zero tangential stress. On the interior surface, at radius  $r_i$ , this results in a high tangential stress and no radial stress.

For the given dimensions, the multiplier effect would

**Figure 9 Thick Walled Cylinder**



result in tangential stresses on the interior surface,  $\sigma_{TWC}$ , being 2.25 times the applied confining stress,  $\sigma_3$ . Conversely, if the confining stress at failure,  $\sigma_f$ , is known, then the theoretical failure stress on the interior surface can be calculated, assuming linear elasticity.

In practice, this theoretical failure stress will exceed the UCS value. The reason for this is that the rock is not linearly elastic, but exhibits some plasticity, especially at stresses near failure (Fig. 9). The “overstress ratio” is defined as the factor by which the TWC failure stress exceeds the theoretical confining stress at failure, assuming the UCS on the inner surface of the TWC and linear elasticity.

The additional benefit of an increased confining stress is an increase in the amount of work done to the sample to fail it. This work is represented by the area under the stress:strain curve. For linear elasticity with brittle failure, the amount of work to failure is small in comparison to that of the triaxial tests’ stress-dependent behaviour. In a practical sense, this would mean that an elasto-plastic material would have considerably more capacity to absorb work energy before failing, therefore predictions made using linear elasticity would be conservative.

**TWC Results.** TWC tests were done on a typical sandstone, a weak sandstone, and a typical mudstone. For each test, the external confining pressure at failure,  $\sigma_f$ , was recorded and the theoretical failure stress on the inside of the TWC,  $\sigma_{TWC}$ , assuming linear elasticity, was calculated. The results were compared to the UCS values to obtain overstress ratios,  $\sigma_{TWC}/\text{UCS}$ . For the sandstone specimens, the TWC test results were 3 to 7 times higher than expected by assuming linear elasticity and the measured UCS values. For the mudstone, this factor was 1.7 to 4.8.

**Increased Strength.** There are reasons for this apparent increase in strength capacity. First, the linearly-elastic prediction of failure is conservative, since the rock on the inner diameter will begin to yield before failure, thus allowing more rock volume to become more highly stressed. In practice, the confining stress at failure for sandstones usually exceeds the linearly elastic prediction by a factor of 2 to 8.

Next, for the TWC tests, the specimen is only experiencing the maximum stress on the inner surface, and not throughout the specimen. Since even “homogeneous” samples have variability in rock strength, the relatively limited amount of the total sample exposed to the maximum stress will reduce the probability that a weakness would be encountered.

**Size Effect.** Similarly, this volumetric effect has an influence on the stability of specimens of various sizes with different inner radii. Smaller specimens will have significantly higher strengths than larger samples. Therefore, the results of laboratory tests may be used directly when considering the stability of perforations, which are the same size, but must be scaled for applicability to wellbore stability.

Laboratory and theoretical work by van den Hoek, et al. (1994)<sup>5</sup> examined the effect of this scale effect on hollow cylinders (HC). For a rock friction angle of  $\phi=30^\circ$ , the scale effect was:

$$\sigma_f \propto (\text{holesize})^{-m} \dots [2]$$

where  $\sigma_f$  = confining stress at failure

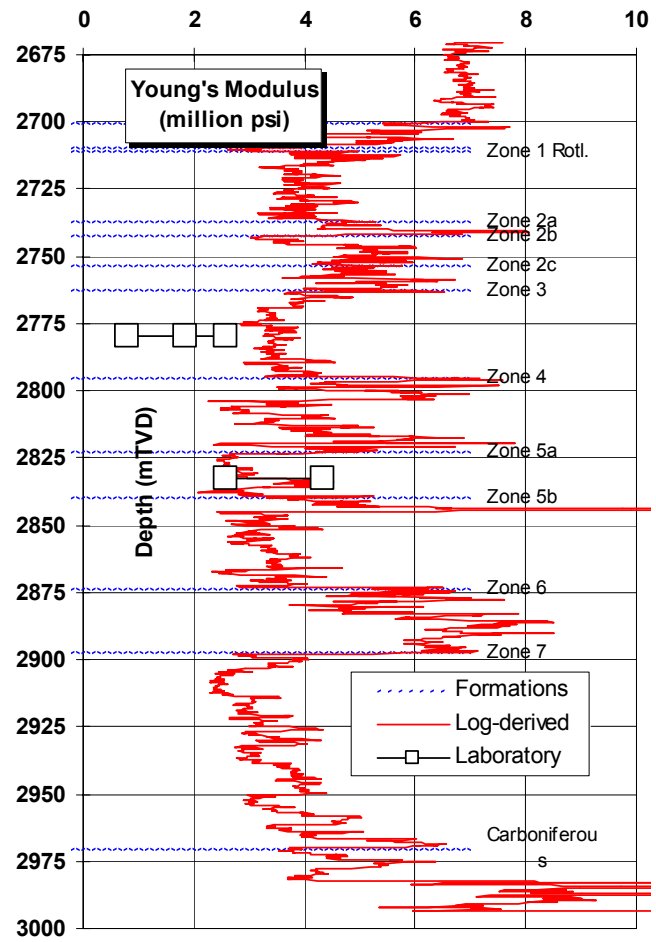
$m = 0.3333$  or  $0.2667$ , depending on the failure mode.

For a drilled diameter of 8.5 inches, this would represent a drop to 39% to 47% of the failure stress of the 0.5 inch inner diameter specimens. In examining their laboratory results for sandstones, drops in strength to 50% to 85% of the laboratory specimens’ strengths were noted. As a result, the collapse pressures for specimens with an inner diameter of 8.5 inches would be 39% to 85% of the laboratory specimen values.

**Triaxial Tests.** Triaxial tests are compressive failure tests conducted on right cylinders of core, tested under a confining stress. While the confining stress can be varied during testing, these specimens were subjected to a constant confining stress. The axial stress was increased to failure.

The effect of the confining stress is to make the samples stiffer, stronger, and more ductile. The strength characteristics are usually described in terms of the Mohr-Coulomb parameters of cohesion and internal friction angle,  $c$  and  $\phi$ . The tests also allow for the measurement of Young’s modulus and Poisson’s ratio,  $E$  and  $v$ .

Figure 10 Young’s Modulus vs. Depth

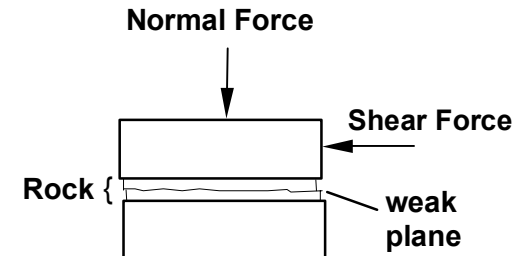


The significance of the triaxial results was that mudstone from the Rotliegend Zone 5a was considerably stronger than the sandstone, and in fact was very strong in terms of its internal friction angle. This implied that this rock would benefit greatly from the support offered by a mud overbalance, provided that the wellbore could be effectively sealed to ensure that the full benefit of the overbalance would be applied to the wellbore.

Laboratory values of Young's modulus are plotted against log-derived values in **Figure 10**. The agreement between the two sources is fair, with a general correlation between the two. Note that the *in situ* confinement would be approximately 2700 psi, therefore the laboratory values at the highest confinement will be most similar to the log-derived values.

**Direct Shear Tests.** After examining the core, it was obvious that the very strong mudstone was weak along the bedding plane. To examine the strength along this plane, the laboratory program was modified to include a direct shear test.

**Figure 11 Direct Shear Test Schematic**



This consisted of cutting a cube of rock with a bedding fault bisecting the specimen. The sample is seated into a split metal box assembly, with a gap between halves at the height of the weak bedding plane, as shown in **Figure 11**. A normal and shear force is applied to the top half of the sample. The shear resistance hits a peak, and the horizontal displacement continues until the residual shear strength is attained.

**Table 2** Triaxial and Direct Shear Test Mohr-Coulomb parameters

| Specimen                   | Test         | c (psi) | $\phi$ |
|----------------------------|--------------|---------|--------|
| Sandstone                  | Triaxial     | 1252    | 38.7°  |
| Mudstone                   | Triaxial     | 721     | 52.9°  |
| Mudstone Bedding, Peak     | Direct shear | 1504    | 15.4°  |
| Mudstone Bedding, Residual | Direct shear | 67      | 13.8°  |

Mohr-Coulomb parameters are summarized in **Table 2**. The bedding plane's cohesion is greater than that of the mudstone. However, any significant displacement along the bedding would destroy its cohesion. The frictional resistance along the bedding is much lower, only  $15.4^\circ$  as compared to the mudstone friction of  $52.9^\circ$ . This has negative implications for mudstone wellbore stability at certain angles.

## Geomechanical Properties from Petrophysical Logs

Petrophysical logs can be used to estimate some geomechanical properties. The benefit of the log-derived method is that it provides continuous properties profiles with

depth. This is useful in delineating differences between near-uniform zones, and in identifying weaker zones. There is also a cost advantage in obtaining these data without having to perform extensive laboratory testing throughout the cored interval.

**Shale Volume**,  $V_{sh}$  of the rock was linearly interpolated between the two extreme values of shaliness detected over the entire logged interval, corresponding to shale and sand units. The gamma ray log was used as a measure of shaliness, although in carbonate sequences the corrected gamma ray is preferred to the gamma ray due to the presence of non-clay radioactive minerals in carbonates.

**Unconfined Compressive Strength.** A value was calculated for the uniaxial compressive strength (UCS) of the rock<sup>6</sup>:

$$a = \frac{2 \cos \phi}{(1 - \sin \phi)} \dots [3]$$

$$UCS = \frac{8.7 \cdot 10^{-9} aE^2}{(1-2\nu)} [0.0045(1-V_{sh}) + 0.008V_{sh}] ..[4]$$

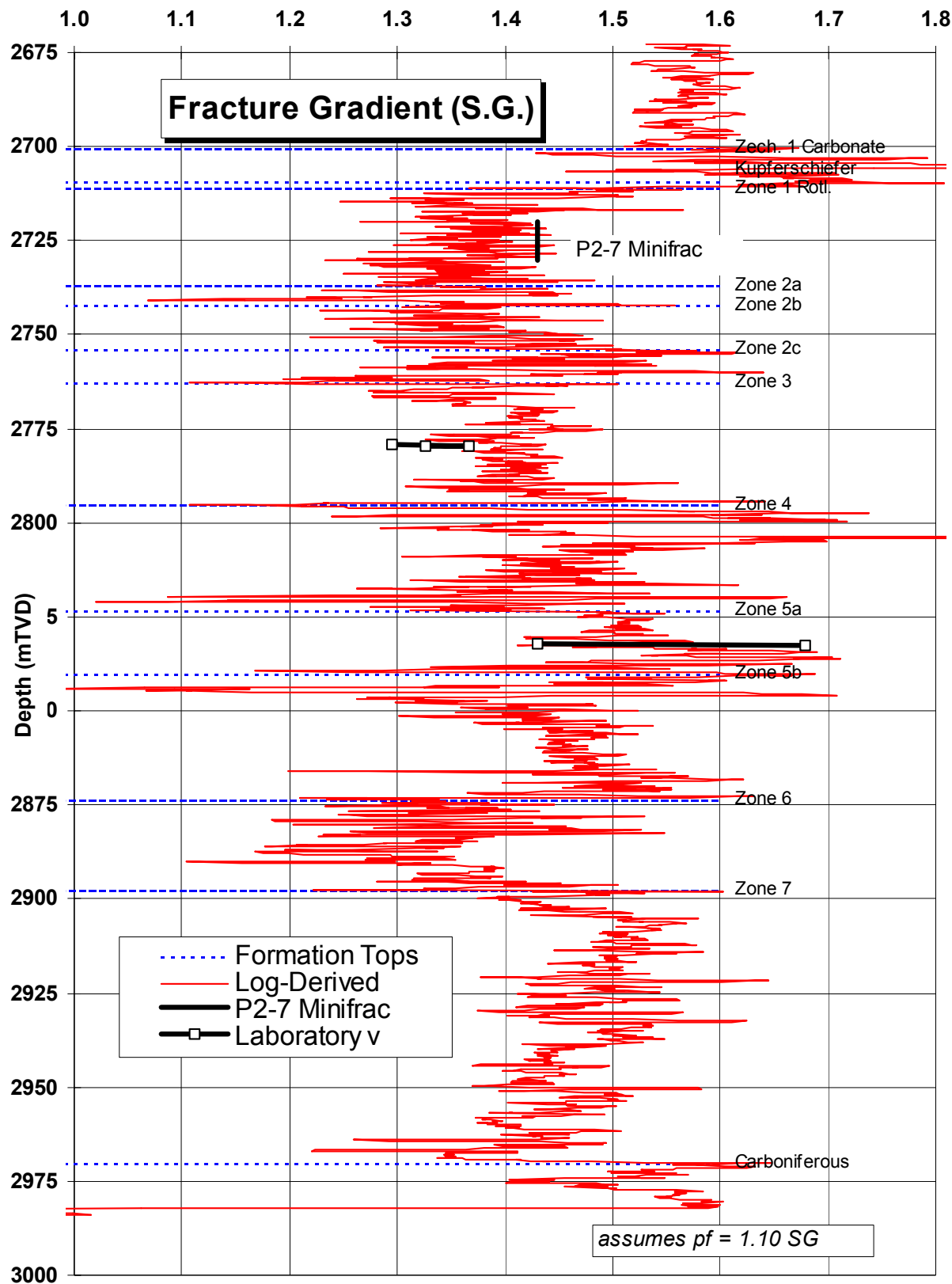
where  $V_{sh}$  is the shale volume of the rock, as interpolated on the basis of the corrected gamma ray response; and  $\phi$  is the internal friction angle for rock, interpolated from  $45^\circ$  to  $25^\circ$  on the basis of  $V_{sh}$ . This will tend to underestimate the strength of Well P2-NE-2 Pilot's anomalously hard mudstone units, of which one interval had a friction angle greater than  $52^\circ$ . However, shales are typically weaker than sandstones, and as the entire logged interval was not cored, it is more reasonable to assume that other shales are weaker.

**Fracture Gradient.** The fracture gradient profile for Well P2-NE-2 Pilot, calculated using Eaton's equation (Eq'n. 1), is shown in **Figure 12**, and shows the depths to the tops of reservoir intervals. The profile assumes a uniform pore pressure of 1.10 SG, therefore this profile will shift to the left with ongoing pressure decline.

The result of the Well P2-7 DST2 minifrac test from the P2-SE reservoir is plotted as a vertical bar in the middle of the Zone 1 Rotliegend unit. This measured fracture gradient of 1.43 SG is higher than the predicted gradient for the same unit in the P2-NE Reservoir. Reservoir pressure gradients were similar (1.09 SG in P2-7 vs. 1.10 SG in P2-NE-2) therefore it is probable that the Poisson's ratio for Zone 1 in P2-7 was slightly higher, thereby resulting in higher horizontal stresses.

Fracture gradients, determined with Eaton's equation and Poisson's ratios obtained from triaxial tests on core specimens, are plotted. Three sandstone samples (~2782mTVD) were tested at different confining stresses: 500, 1500, and 3500 psi, which would result in different degrees of ductility during testing. Since the effective confining stress at this depth was ~2700 psi, the tests at the highest two values of  $\sigma_3$  would be most representative. In **Figure 12**, these correspond to the right and centre points, respectively. Taking an average of these two values gives a fracture gradient of 1.35 SG, which is on the low side of the range 1.35-1.45 SG seen in the log-derived plot for this same depth.

Figure 12 Fracture Gradient for Well P2-NE-2 Pilot



Similar results are plotted for mudstone at 2835mTVD. Two specimens were tested at confining pressures of 500 and 1500 psi. The observed Poisson's ratios were 0.325 and 0.216 (respectively) although the value of 0.216 was of questionable quality. These Poisson's ratios are higher than for the sandstone, consequently the fracture gradients are higher: 1.68 and 1.43 SG. This is in fair agreement with the log-derived fracture gradient, which has a high variance at this depth.

The stress contrasts are important when considering containment of hydraulic fracture stimulations, and the log-derived profile provides an important planning tool for fracture placement. The profile in **Figure 12** is representative of the actual stress contrasts and should be considered when planning any fracture stimulation in this field.

#### Limitations to Log-Derived Properties.

1. The log-derived properties are largely based on sonic data, and as these are measurements of micro-deformations they may not always be applicable to large-scale deformations. Fjaer, et al. (1992)<sup>7</sup> note that the dynamic moduli are significantly higher than static moduli. In particular, where the rock has any strain-dependent properties, as would be the case for lightly-cemented clastic rocks, the log-derived properties may not be representative of the rock undergoing larger strains, as would be expected during drilling or drawdown conditions.
2. The derived properties are based on several broad correlations with density, sonic velocity, and shale volume. As such, there will be some difference between the predicted and actual properties. Therefore, it is essential to conduct a limited number of laboratory tests to calibrate the log-derived predictions. In general, the log-derived values should be scaled to match the laboratory results.
3. The log-derived properties rarely take account of rock property anisotropy. Sedimentary rocks in particular have an internal structure that is due to their depositional and post-depositional environments. Typically, sedimentary rocks have orthotropic properties, with properties in the horizontal plane varying significantly from those in the vertical direction. Where rock anisotropy is an issue, the anisotropy should be considered.
4. The interpretation of data often involves the use of models or assumptions that are not explicitly stated or are not justified. The prediction of horizontal stress, as an example, involves the use of Eaton's model that assumes zero lateral strain. In a quiescent basin, this is a good approximation of the existing stress state. However, in heavily faulted fields, or even adjacent to a single fault, this assumption may result in unrepresentative predictions. Furthermore, assumptions of pore pressure distributions must be made and these may not be well known.

#### Wellbore Stability

After the wellbore is drilled into the rock, the *in situ* stresses in the rock mass are re-directed around the wellbore, resulting in stress concentrations. These become more extreme as the two principal stresses, acting perpendicular to the wellbore, become more unequal. The resultant stress concentrations

around the wellbore lead to a constriction in the mud weight window between the conditions of wellbore collapse and mud losses.

**Stress Concentrations around a Wellbore.** The magnitudes of these stresses can be calculated using the Kirsch equations<sup>7</sup>, assuming that the wellbore is circular; the mudcake is 100% effective (i.e. no filtration into the formation); and, the rock is linearly elastic

The portion of the total stresses borne by the rock matrix, as opposed to the formation fluids, are known as the *effective stresses*, i.e. the total stresses minus the formation fluid pressure<sup>8</sup>. These stresses are related as follows:

$$\sigma' = \sigma - p_f \dots [5]$$

where:

$\sigma'$  is the effective stress

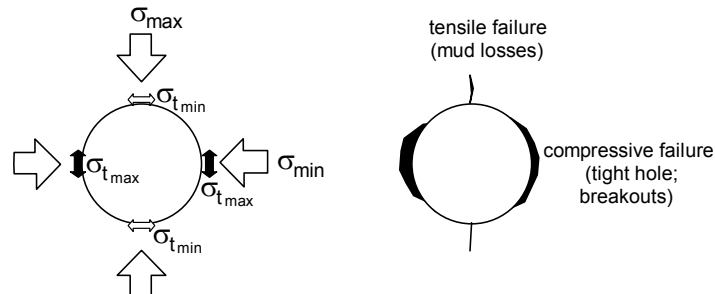
$\sigma$  is the total stress

$p_f$  is the pore pressure

For wellbore stability, the most important stresses are the effective stresses, since these are the stresses borne by the rock matrix itself. Where these stresses are greater than the rock's compressive or tensile strengths, wellbore failure or fracture will occur.

The stress distributions away from the wellbore are complex for a non-uniform stress field, and are a function of the position around the wellbore. At the wellbore wall the radial stress is uniform and equal to the mud pressure, while the tangential stresses at the wellbore wall are the most extreme parallel to the minor and major stresses. Under certain circumstances, tensile failure or compressive failure may occur (**Figure 13**).

**Figure 13 Stresses around the Wellbore and their Consequences**



If the rock is assumed to be homogeneous, isotropic, and linearly elastic, and the well is drilled in any principal stress direction, the magnitudes of the maximum and minimum effective tangential stresses at the wellbore are<sup>9</sup>:

$$\sigma'_{t\min} = -\sigma_{\max} + 3\sigma_{\min} - p_{\text{mud}} - p_f \dots [6]$$

$$\sigma'_{t\max} = 3\sigma_{\max} - \sigma_{\min} - p_{\text{mud}} - p_f$$

where:

$\sigma'_{t\min}$  = minimum tangential stress (effective)

$\sigma'_{t\max}$  = maximum tangential stress (effective)

$\sigma_{\max}$  = maximum stress, perpendicular to the wellbore

$\sigma_{\min}$  = minimum stress, perpendicular to the wellbore

$p_{\text{mud}}$  = wellbore mud pressure

$p_f$  = formation fluid pressure

If the rock's tensile strength is assumed to be negligible, Equations 6 can be rearranged to obtain limits to the mud weight window:

$$\begin{aligned} p_{mud} &\leq -\sigma_{max} + 3\sigma_{min} - \sigma'_{t\ min} - p_f \\ p_{mud} &\geq 3\sigma_{max} - \sigma_{min} - \sigma'_{t\ max} - p_f \end{aligned} \quad ...[7]$$

where  $p_{mud}$  = wellbore mud pressure =  $(z^*ECD)$ , consisting of both static and dynamic components.

**Stability Analysis of P2-NE Field Sandstone.** The results of the analysis are presented in **Figure 14** where the stability values have been plotted in plan view as a colour-scale "dartboard" of stability values. These values have been discretized to increments of 10° for azimuth and inclination.

The centre point represents a vertical well, with every concentric circle representing a 10° increment of inclination. At the limit, the perimeter of the circle represents all horizontal well trajectories. North is at the top of the circle. The two large arrows at the circle's perimeter indicate the orientation of the major horizontal stress. A solid arrow points in an azimuth of 150°, representing the Well P2-NE-2 Horizontal azimuth. The blue areas represent more stable trajectories than the red areas. Input variables are listed in **Table 3** and **Table 4**.

The figure shows the stability of wells with a 10.4ppg (1.25 S.G.) and 10.6ppg (1.27 S.G.) mud weight. In stability terms, the vertical well is arbitrarily assigned a value of "1.00" and all other trajectories are shaded relative to that. The worst stability value is 0.45 and this occurs around the perimeter (i.e. a horizontal well), particularly in the north-west and south-east quadrants. The "0.45" means that the rock strength required to ensure stability must be 1.00/0.45 times the rock strength required for a vertical well. In practical terms, the mud weight should be increased if there is insufficient rock strength, and the new stability values examined.

Inclined wells lose their relative stability very quickly with inclination, reaching 60% stability with only a 45° inclination. This is due to the fairly high overburden gradient for an offshore field of 1.00 psi/ft, the minimum horizontal stress gradient of 0.61 psi/ft, and the fact that the reservoir is slightly overpressured at 1.10 SG. The best azimuths are towards the NE and SW.

Fortunately, the requirement for rock strength is not excessive. With a mud weight of 10.4ppg (1.25 S.G.), the minimum rock strength needed for a vertical well is 3120 psi, based on a linear elastic stress analysis, which overpredicts the need for rock strength. If the results of the TWC tests are examined and the minimum overstress ratio of 3.0 is reduced by 50% due to specimen scale effects (viz. Eq'n. 2), the rock strength required could be reduced by a factor of 1.5 to attain  $3120\text{psi}/3.4= 2064$  psi. This is less than the vast majority of UCS values (Fig. 8), therefore the mud weight should be adequate. Certainly, the P2-NE-2 Pilot well was drilled at an inclination of 55° with a mud weight of 1.25 SG throughout the reservoir without adverse effects.

The difference between a 55° inclination and a 90° inclination does not appear to be great: relative stabilities are 0.54 vs. 0.46, respectively, or a drop of 17% in relative terms. If the mud weight is increased to 1.27 SG (**Figure 14; lower half**) the required rock strength drops from 3120 psi to 2621 psi, or 1741 psi when factored. This is a reduction of 16%, and should compensate for the 17% difference between the 55° and horizontal inclinations.

It was recommended that the P2-NE-2 Horizontal well be drilled with a mud weight of 1.25 SG at an inclination of 55°, and with 1.27 SG for a horizontal inclination.

**Stability Analysis of P2-NE Field Mudstone.** The results of the analysis are presented in **Figure 15** where the stability values have been plotted in plan view as a colour-scale "dartboard" of values, as per Figure 14. **Figure 15** also shows the stability of wells with a 10.4ppg (1.25 S.G.) and 10.6ppg (1.27 S.G.) mud weight.

The mudstone does not appear to be problematic. This is despite the fact that a conservative mudcake efficiency of 50% was used in the analysis, meaning that the wellbore wall had filtrate invasion to result in a pore fluid pressure midway between the wellbore pressure and the reservoir pressure. The mudstone UCS values are far in excess of any required rock strength, therefore the effect of inclination and azimuth are inconsequential. As a result, the mud weight recommendations for the sandstone are adequate for the mudstone. However, good drilling practice was recommended to prevent shocking the well with pressure swabs or surges, possibly resulting in instabilities.

**Effect of Weaker Bedding Planes.** The laboratory tests found that the mudstone samples were exceedingly strong, but that there was an inherent weakness in the mudstone along the bedding. Here, the frictional parameters for cohesion and friction,  $(c,\phi)$  were (1504 psi, 15.4°) compared with (721 psi, 52.9°) for the mudstone itself. Despite the high value of cohesion along the plane, the lower friction angle reduces the beneficial effect of a mud overbalance for the weak plane versus the rest of the mudstone.

The effect of this on wellbore stability is more difficult to determine. Where the well penetrates the bedding at right angles, there is no effect at all, since shear forces along the plane should be negligible. As the well inclination increases, or as the bedding inclination increases, the well intersects the bedding at an ever-increasing obtuse angle. This increases the shear forces acting on the weak plane. At even higher angles of inclination, the weak plane has less of an effect since the well is parallel to the bedding and shear forces are smaller. For a high-angle well in the P2-NE Reservoir, the minimum well strength will be roughly at a well inclination of 60°–80°. This is shown graphically in **Figure 16**, in which the stability along the weak plane is shown, relative to the stability through the intact mudstone. For a horizontal bedding plane, this becomes the weaker part of the mudstone after an inclination of 55°. Fortunately, the drop in stability is not great and is fairly constant for higher inclinations.

Figure 14 P2-NE Reservoir Sandstone Stability

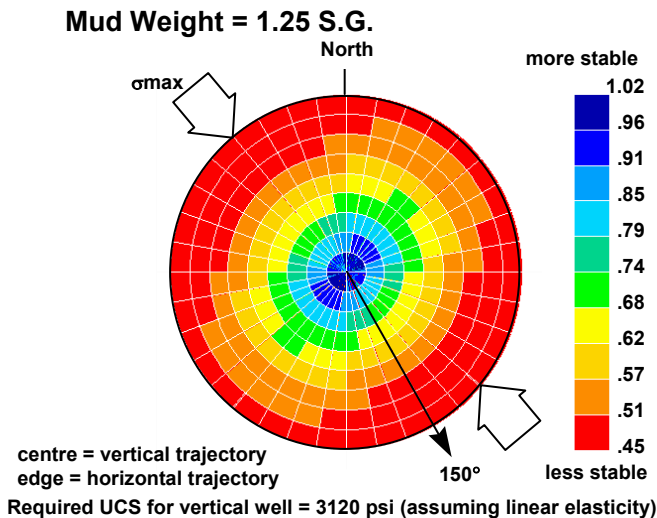
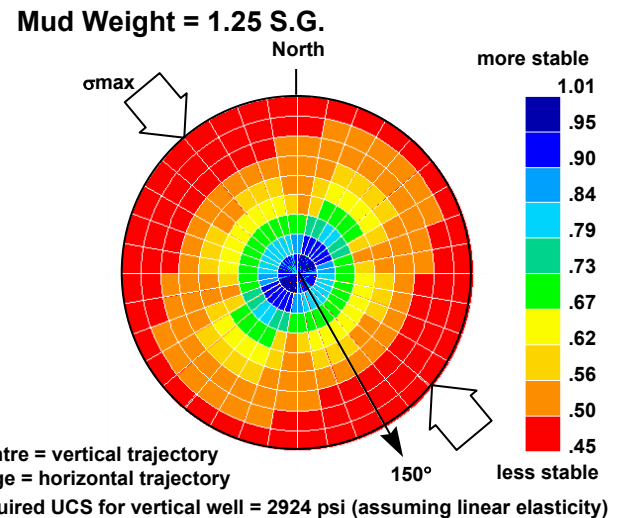
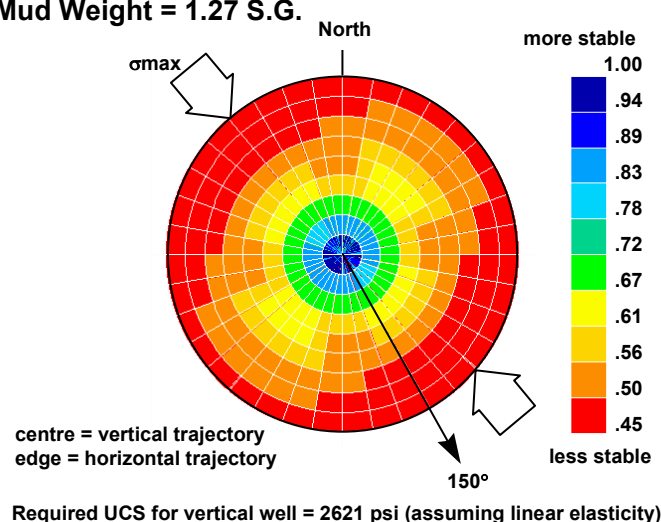


Figure 15 P2-NE Reservoir Mudstone Stability



Mud Weight = 1.27 S.G.



Mud Weight = 1.27 S.G.

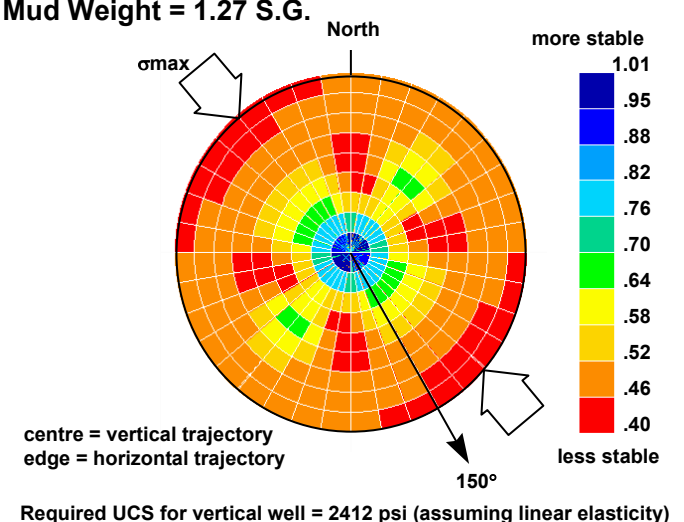


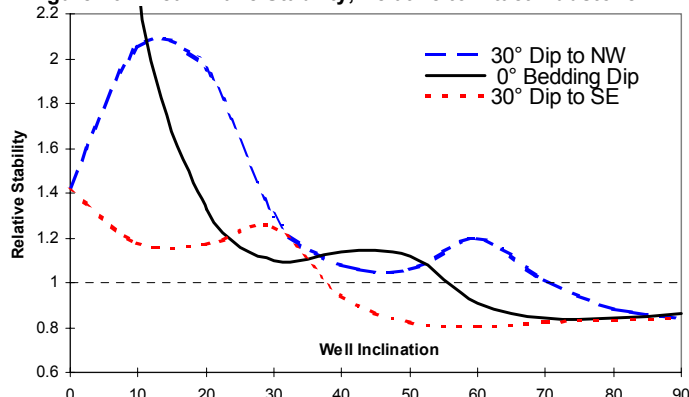
Table 3 Stress Parameters for Stability Analysis

| Variable                  | Symbol          | Gradient    | Pressure |
|---------------------------|-----------------|-------------|----------|
| vertical stress           | $\sigma_v$      | 1.00 psi/ft | 9000 psi |
| maximum horizontal stress | $\sigma_{\max}$ | 0.75 psi/ft | 6750 psi |
| minimum horizontal stress | $\sigma_{\min}$ | 0.61 psi/ft | 5490 psi |
| formation fluid pressure  | $p_f$           | 0.48 psi/ft | 4320 psi |

TVD = 9000 ft = 2743 m

Table 4 Rock Parameters for Stability Analysis

| Variable           | Sandstone | Mudstone |
|--------------------|-----------|----------|
| Tensile strength   | 0         | 0        |
| Friction Angle     | 38.7°     | 52.9°    |
| Poisson's Ratio    | 0.16      | 0.325    |
| Mudcake Efficiency | 100%      | 50%      |

**Figure 16 Weak Plane Stability, Relative to Intact Mudstone**

Where the folding of the rock has resulted in the tilting of the bedding, the stability changes. Where the bedding dips in the same direction as the well trajectory ("30° Dip to SE") the angle of incidence between the well and the bedding plane is lower and so the stability is lower. Conversely, where the bedding is tilted to the north-west, the well is actually more stable at a small angle of well inclination: this is because the well intersects the bedding plane at closer to a perpendicular angle. The three curves are similar, with a phase-shift between the three cases of bedding dip; the reason that they are not identical is because the vertical and horizontal stresses have not rotated.

No wellbore stability issues were expected below well inclinations of 45°. This is because the bedding will tend to dip NW over the early part of the P2-NE-2 Horizontal Well build section. The remainder of the well may intersect horizontally-bedded mudstone, until the very end of the well where the bedding dips SE. Here, the stabilities converge to approximately 85% of the stability of the intact material. Given the high strength of the intact mudstone, wellbore instability is not expected. Stability requires good mud design to ensure that the full benefit of the mud overbalance is applied to the wellbore, and good drilling practice.

## Conclusions

The geomechanics study indicated that Well P2-NE-2 Horizontal should remain stable during drilling, provided that the mud weight was increased to 1.27 SG. The vertical stress gradient in the P2-NE reservoir is 1.0078 psi/ft. This value was for Well P2-4 at a depth of 2720mTVD within the reservoir. The vertical stress gradient will be lower in shallower intervals due to the lower degree of rock compaction and because the offshore location results in much lower vertical stress gradients at shallow depths.

The fracture pressure gradient varies from 1.3 to 1.6 SG, based on a log-derived analysis. Variations in this gradient are representative of the actual variations within the reservoir. These predictions are in fair agreement with laboratory and minifrac results. The Rotliegend Zone 1 fracture pressure was measured in Well P2-7, P2-SE reservoir, and was found to be 6600-6800 psi. The test provided a definite measure of the fracture gradient within the reservoir, and its value is

indicative of the fracture gradient (minimum horizontal stress) to be expected in the P2-NE Reservoir.

The orientation of the maximum horizontal stress (i.e. fracture extension orientation) is 130°-310° (NW-SE). Any induced hydraulic fractures will propagate in this orientation. The borehole breakout evidence for a consistent NW-SE maximum horizontal stress orientation is convincing, and is in agreement with the strike of nearby normal faults and the regional North Sea stress trend. The orientation of the maximum horizontal stress determined from residual strain relaxation tests was 112°. This result is less compelling than the borehole breakout results, but is in fair agreement with them. The core method provides an alternative method of stress direction determination where breakout information is unavailable or ambiguous.

The reservoir sandstones are homogeneous, but are often weak. Unconfined compressive strengths were as low as 800 psi, with typical strengths over 2,000 psi. Stability problems while drilling were not anticipated, assuming that adequate mud weight was used and good drilling practice was observed.

The reservoir mudstones are anisotropic due to weaker strength along bedding, but are much stronger than the sandstones. Unconfined compressive strengths of 5,000 psi to 15,000 psi were observed for the one zone tested, and good correlation with the log-derived profile indicates that these rocks will not be problematic during drilling. There is a good correlation between rock strength and the gamma ray response.

Thick-walled cylinder tests show that the sandstones have significantly more strength capacity than would be predicted with linear elastic models.

Stability of an 8.5" wellbore is roughly half that of a 0.5" perforation. This scale effect means that rock strengths around an open-hole or slotted liner completion would have to be double that of cemented perforated completions to have a simultaneous sandstone failure during drawdown. Where rock strengths are indicative of marginal sand production potential, this might have affected completion selection. However, with the weak zones seen here, sanding potential is probable regardless of the completion.

## Recommendations

For drilling Well P2-NE-2 Horizontal, it was recommended that mud weights be increased from the current 1.25 SG at a 55° inclination, to 1.27 SG at the 90° inclination. Note that this was significantly less than the 1.34 SG anticipated to be necessary for a horizontal well. This also assumed that the resultant mud overbalance would be fully applied to the wellbore by using a mud chemistry that quickly sealed the low permeability mudstones. (A mudcake efficiency of 50% was used in the mudstone stability analysis.) Sandstones are less problematic due to the ease of forming a filtercake.

Mud weights should be increased at the onset of instability. When wellbore instabilities have the potential to interfere with drilling operations, mud weights should be increased in increments of approximately 0.01 SG until the wellbore

stabilises. It is always easier to protect wellbore stability by increasing mud weights at the onset of problems than it is to re-establish stability after severe problems.

Equivalent circulating densities (ECDs) must not exceed the fracture gradient. Higher ECDs will result in wellbore fracture and a degradation of wellbore stability. This is particularly problematic for long horizontal wells where the requirement for hole cleaning increases the need for hydraulic cleaning and therefore higher pumping pressures. Good drilling practice, such as rotating the drillstring to agitate and entrain cuttings, should be used. Circulating the wellbore adequately before tripping will minimise resistance during tripping out or running in, thus avoiding the occurrence of stuck pipe.

Care should be taken when tripping in weaker sandstone zones. Surge and swab pressures associated with rapid string movements may momentarily reduce the supporting mud overbalance. This may result in sudden instabilities in these weaker rocks.

Core should always be examined when conducting wellbore stability analyses. While log-derived geomechanical properties have their advantages, only a careful examination and testing of core can provide calibration of the log-derived profiles. Critical features, such as the weak bedding plane within the mudstone found in this study, are not evident from the log-derived properties.

## Epilogue

Encouraged by the geomechanics report, the drilling team proceeded to drill the P2-NE-2 Horizontal well with a mud weight of 1.25 SG, much less than the 1.34 SG previously anticipated, and slightly under the 1.27 SG recommended. No wellbore stability problems were reported.

## Acknowledgements

The author would like to thank Clyde Petroleum Exploratie B.V.; Dyas B.V.; GDF Participation Nederland B.V.; Oranje Nassau Energie B.V. and Energie Beheer Nederland, for permission to publish this paper. The assistance of Mr. Wouter d'Engelbronner and Mr. Keith Mustard was especially appreciated. Credit for the exemplary laboratory work is due Fractech Ltd., Middlesex, and Imperial College, London, U.K.

## Nomenclature

|           |                                  |
|-----------|----------------------------------|
| $E$       | = Young's modulus                |
| ECD       | = equivalent circulating density |
| $m$       | = exponent                       |
| $V_{sh}$  | = shale volume [fraction]        |
| $\nu$     | = Poisson's ratio                |
| $p_f$     | = formation pore pressure        |
| $p_{mud}$ | = wellbore mud pressure          |
| $r_i$     | = TWC, interior radius           |
| $r_o$     | = TWC, exterior radius           |
| $\sigma'$ | = effective stress               |
| $\sigma$  | = total stress                   |

|                     |   |
|---------------------|---|
| $\sigma_f$          | = failure stress  |
| $\sigma_f^{actual}$ | = confining stress at failure, measured in TWC test   |
| $\sigma_f^{L.E.}$   | = confining stress at failure, theoretical value back-calculated from UCS values, in TWC test |
| $\sigma_h$          | = horizontal stress (i.e., fracture gradient)   |
| $\sigma_{max}$      | = maximum total stress perpendicular to the wellbore  |
| $\sigma_{min}$      | = minimum total stress perpendicular to the wellbore  |
| $\sigma'_{t_{max}}$ | = maximum tangential stress (effective stress)  |
| $\sigma'_{t_{min}}$ | = minimum tangential stress (effective stress)  |
| $\sigma_{TWC}$      | = tangential stress inside thick-walled cylinder stress                                       |
| $\sigma_v$          | = vertical stress   |
| $\sigma_3$          | = confining stress, or minimum principal stress   |
| $\propto$           | = "is proportional to"  |
| $\sim$              | = "approximately"   |

## References

- 1) Eaton, B.A. (1969) "Fracture Gradient Prediction and Its Application in Oilfield Operations", SPE2163, *JPT* 21, pp.1353-1360
- 2) Addis, M.A., Last, N.C., and Yassir, N.A. (1984) "The estimation of horizontal stresses at depth in faulted regions and their relationship to pore pressure variations", proc. Eurock'94 SPE/ISRM Int'l. Conf. Rock Mechanics in Petroleum Engineering, 29-31 Aug. 1994, Delft, the Netherlands, pp.887-895.
- 3) Kunze, K. R. and R. P. Steiger (1991) "Extended leakoff tests to measure in situ stress during drilling", proc. 32nd U.S. Symp. on Rock Mechanics, Rock Mechanics as a Multidisciplinary Science, ed. J.-C. Roegiers, Norman, Oklahoma, pp.35-44.
- 4) Kunze, K. R. and R. P. Steiger (1992) "Accurate In Situ Stress Measurements During Drilling" Operations, SPE 24593, SPE ATCE, Oct 4-7, 1992, Washington, D.C., pp. 491-499.
- 5) Van den Hoek, P.J., D.-J. Smit, A.P. Kooijman, Ph. De Bree, C.J. Kenter, M.Khodaverdian (1994) "Size dependency of hollow-cylinder stability", SPE28051, Proceedings, Eurock'94 SPE/ISRM International Conference, Rock Mechanics in Petroleum Engineering, 29-31 August, Delft, pp.191-198
- 6) Bruce, S. (1990) "A Mechanical Stability Log", IADC/SPE19942, proc. IADC/SPE Drilling Conf., Houston, TX, Feb 27-Mar. 2, 1990, pp.276-281.
- 7) Fjaer, E., Holt, R.M., Horsud, P., Raaen, A.M., Risnes, R. (1992) *Petroleum related rock mechanics*, Developments in Petroleum Science series, no. 33; publ. Elsevier, Amsterdam, 338 pp.
- 8) Terzaghi, K. (1943) *Theoretical Soil Mechanics*, publ. John Wiley and Sons, Inc., 510pp.
- 9) Jaeger, J.C. and Cook, N.G.W. (1976) *Fundamentals of Rock Mechanics*, 2<sup>nd</sup> ed., publ. Chapman and Hall, London, 585pp.

## Metric Conversion Factors

|          |   |
|----------|---|
| 1 ft     | = 0.3048 metre                            |
| 1 psi    | = 6.8947 kPa                              |
| 1 psi/ft | = 22.62 kPa/m                             |
| 1 SG     | = 1.00 g/cm <sup>3</sup><br>= 8.34543 ppg |